

# Stochastic approach to modeling photoresist development\*

Chris Mack<sup>a)</sup>

1605 Watchhill Road, Austin, Texas 78703

(Received 25 June 2008; accepted 16 March 2009; published 11 May 2009)

In this paper a continuous approximation to the critical ionization (CI) model has been derived and shown to match the CI model extremely closely. Further, both of these models were shown to match the widely used Mack model of dissolution over the lithographically significant ranges of development rates. The variance of the dissolution rate is shown to arise from the variation in the development path required to bypass randomly insoluble polymer molecules rather than just the variance in the polymer solubility itself. Percolation theory, where the percolation probability is equal to the probability that a polymer molecule will become soluble, has the potential for providing the theoretical framework required to determine this variance in dissolution path. © 2009 American Vacuum Society. [DOI: 10.1116/1.3117346]

## I. INTRODUCTION TO STOCHASTIC MODELING

Most theoretical descriptions of lithography make an extremely fundamental and mostly unstated assumption about the physical world being described: the so-called *continuum approximation*. Even though light energy is quantized into photons and chemical concentrations are quantized into spatially distributed molecules, the descriptions of aerial images and latent images ignore the discrete nature of these fundamental units and use instead continuous mathematical functions. When describing lithographic behavior at the nanometer level, an alternate approach, and in a very real sense a more fundamental approach, is to build the quantization of light as photons and matter as atoms and molecules directly into the models used. Such an approach is called *stochastic modeling*, and involves the use of random variables and probability density functions to describe the statistical fluctuations that are expected. Of course, such a probabilistic description will not make deterministic predictions; instead, quantities of interest will be described by their probability distributions, which in turn are characterized by their moments, such as the mean and variance.

Stochastic modeling of lithography offers two advantages over continuum modeling. First, since all fundamental mechanisms involved with lithographic printing are necessarily atomistic and stochastic in nature, any attempt to develop first-principles models should at least consider the stochastic nature of these first principles. Second, a continuum model is fundamentally incapable of predicting line-edge roughness (LER), since that roughness comes from the stochastic nature of the events that give rise to a lithographic feature. In this paper, the stochastic nature of resist dissolution is explored. First the previously published critical ionization model is described, then a continuous approximation to this model is derived. The uncertainty in polymer dissolu-

tion is considered, but the uncertainty in development rate requires a stochastic description of the development path as well.

## II. CRITICAL IONIZATION MODEL

Tsiartas *et al.*<sup>1</sup> developed the first truly mechanistic model of phenolic polymer-based photoresist dissolution called the *critical ionization* (CI) model. Consider a resist made up of monodisperse phenolic polymers each with  $N$  phenol groups, some of which are initially blocked (protected). Acid generated upon exposure catalyzes the deblocking (deprotection) of these phenol groups during postexposure bake. Exposure of an unblocked site to developer leads to ionization of the phenol  $-OH$  group. The polymer becomes soluble in the developer only after some critical fraction of the  $N$  phenol groups become ionized. Suppose that  $k$  phenol groups must be ionized before the polymer becomes soluble. The critical ionization fraction,  $\phi_{crit}$ , is then

$$\frac{k-1}{N} < \phi_{crit} \leq \frac{k}{N}. \quad (1)$$

Given some probability  $p_{ion}$  that a given phenol group is ionized, the probability that  $j$  of the  $N$  phenol groups on any given polymer are ionized is given by the binomial distribution (assuming that each ionization event is independent). The probability that a polymer molecule is soluble is just the sum of all of these binomial probabilities for  $j \geq k$ . Defining a random binary variable  $y_r$  ( $y_r=1$  when the polymer is soluble and  $y_r=0$  when not), the result of Tsiartas *et al.*<sup>1</sup> is

$$P(y_r = 1) = \sum_{j=k}^N \frac{N!}{(N-j)!j!} (p_{ion})^j (1-p_{ion})^{N-j}. \quad (2)$$

A simplified version of this critical ionization model is frequently invoked (informally dubbed “critical ionization lite”). Ignoring the details of phenol group ionization, one can idealize the dissolution process by assuming that whenever a polymer touches the resist-developer interface, all unprotected phenol groups are instantly ionized. Thus, for any polymer on the resist-developer interface,  $p_{ion}$  can be related

\*This paper was presented at the 52nd International Conference on Electron, Ion, and Photon Beam Technology & Nanofabrication Conference, Portland, OR, May 27–30, 2008.

<sup>a)</sup>Electronic mail: chris@lithoguru.com

to the probability that a site will still be blocked at the end of the postexposure bake ( $p_m$ ):  $p_{\text{ion}} = 1 - p_m$ . Further, the probability  $p_m$  can be related to the mean concentration of blocked polymer sites at the end of the PEB,  $\langle M \rangle$ , and the total concentration of phenol groups (blocked and unblocked), Ph. If the resist is formulated so that  $l$  of the  $N$  phenol groups are initially blocked,

$$\frac{\text{Ph}}{M_0} = \frac{N}{l} \text{ and } p_m = \langle m \rangle \frac{l}{N}, \quad (3)$$

where  $M_0$  is the initial (before deprotection) concentration of blocked polymer sites, and  $m$  is the relative concentration of blocked polymer sites,  $M/M_0$ .

If one makes the assumption that the dissolution rate of the photoresist is proportional to the probability that a given polymer molecule is soluble, the critical ionization model (lite) leads to a development model: the prediction of dissolution rate  $R$  as a function of mean concentration of remaining blocked polymer sites.

$$\begin{aligned} \langle R \rangle &= R_{\text{max}} P(y_r = 1) \\ &= R_{\text{max}} \sum_{j=k}^N \frac{N!}{(N-j)! j!} \left(1 - \langle m \rangle \frac{l}{N}\right)^j \left(\langle m \rangle \frac{l}{N}\right)^{N-j}. \end{aligned} \quad (4)$$

The assumption that dissolution rate is proportional to the polymer solubility probability will be explored below. Often, a minimum dissolution rate ( $R_{\text{min}}$ ) is added to Eq. (4) to account for the small but nonzero dissolution rate of completely protected polymer.

### III. NEW FORMS OF THE CRITICAL IONIZATION MODEL

The critical ionization model expressed in Eq. (4) is reasonably inconvenient to use in a simulation program (factorials are computationally expensive). Since  $N$  is reasonably large (typical values are between 10 and 30), one can approximate the binomial probability density function with a Gaussian and the summation with an integral:

$$R = \frac{R_{\text{max}}}{\sqrt{2\pi}\sigma_j} \int_{k-0.5}^N e^{-(j-\langle j \rangle)^2/2\sigma_j^2} dj, \quad (5)$$

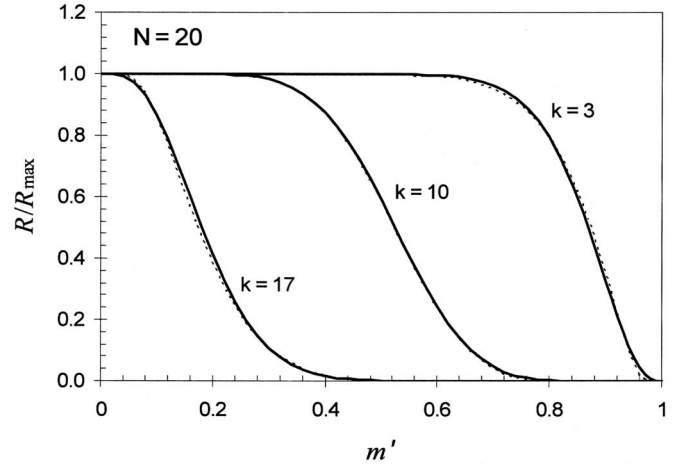
where

$$\langle j \rangle = N \left(1 - \langle m \rangle \frac{l}{N}\right), \quad \sigma_j = \sqrt{N \left(1 - \langle m \rangle \frac{l}{N}\right) \left(\langle m \rangle \frac{l}{N}\right)}.$$

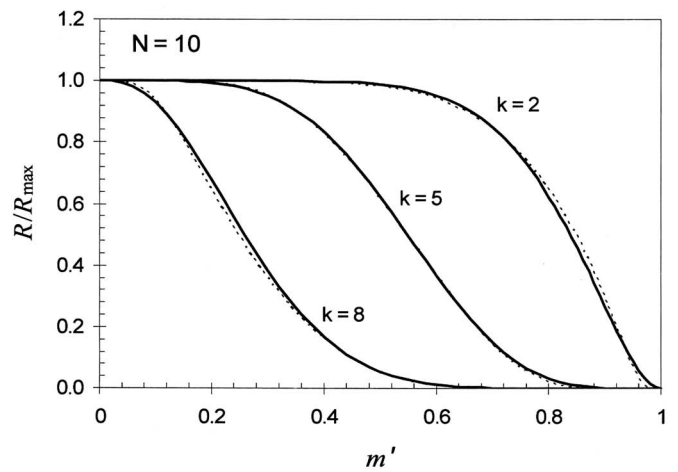
Note that in converting the summation to an integration, a starting point for integration of  $k-0.5$  is chosen as the midpoint between the discrete intervals of the summation [i.e.,  $\phi_{\text{crit}}$  is chosen as the midpoint of the range given by Eq. (1)]. Carrying out the integration gives

$$R = \frac{R_{\text{max}}}{2} \operatorname{erfc} \left( \frac{k-0.5-\langle j \rangle}{\sqrt{2}\sigma_j} \right), \quad (6)$$

where  $\operatorname{erfc}$  is the complimentary error function. Setting this expression in terms of the relative concentration of blocked polymer sites,



(a)



(b)

FIG. 1. Comparison of the critical ionization model of Eq. (4) (solid lines) with its approximate continuous version from Eq. (7) (dotted lines) for different values of  $k$ : (a)  $N=20$  and (b)  $N=10$ . Note that for the case of  $k=N/2$ , the dotted and solid lines are indistinguishable.

$$R = \frac{R_{\text{max}}}{2} \operatorname{erfc} \left( \sqrt{\frac{N}{2}} \frac{(\langle m \rangle - m_{th})}{\sqrt{\langle m \rangle \left(\frac{N}{l} - \langle m \rangle\right)}} \right), \quad (7)$$

where

$$m_{th} = \frac{N-k+0.5}{l}.$$

Equation (7) can be termed the continuous approximation critical ionization (CACI) model.

Figure 1 shows several comparison plots of CI and CACI models. The CACI model does a better job of matching the CI model for higher values of  $N$  and for values of  $k$  nearer  $N/2$ . In general, though, the continuous approximate form should be more than adequate for most simulation applica-

tions. If a minimum development rate is added to the right hand side of Eq. (7), this model will have five parameters:  $R_{\max}$ ,  $R_{\min}$ ,  $l$ ,  $N$ , and  $m_{\text{th}}$  (or alternatively  $k$ ).

An advantage of the CI or the CACI models is the relationship between several of the model parameters ( $k$ ,  $l$ , and  $N$ ) and formulation/structural parameters of the resist molecules themselves. More empirical dissolution models, however, are used in lithography simulators. The most popular of these has been called the original Mack dissolution model,<sup>2</sup> derived based on a proposed kinetic dissolution mechanism:

$$R = R_{\max} \frac{(a+1)(1-m)^n}{a+(1-m)^n} + R_{\min}, \quad (8)$$

where

$$a = \frac{n+1}{n-1} (1-m_{\text{th}})^n.$$

This four parameter model has been found to match experimental dissolution-rate data quite well. Figure 2 shows a few examples how of this semiempirical kinetic model compares to the critical ionization model (with  $R_{\min}=0$ ). The comparison was made by finding the Mack model parameters  $n$  and  $m_{\text{th}}$  that best fit the CI model for  $R < R_{\max}/2$ . Since the two models do not closely match over the full range of development rates, fitting to the lower development rates is preferred since higher development rates have much less impact on resist profile formation.

Figure 3 shows the resulting best fit Mack dissolution selectivity parameter  $n$  over a wide range of  $k$  values for both  $N=10$  and  $N=20$  (for convenience,  $l=N$  was chosen). Empirically, the best fit Mack model parameters can be related to the CI parameters by

$$m_{\text{th}} = 1 - \frac{k-1}{N},$$

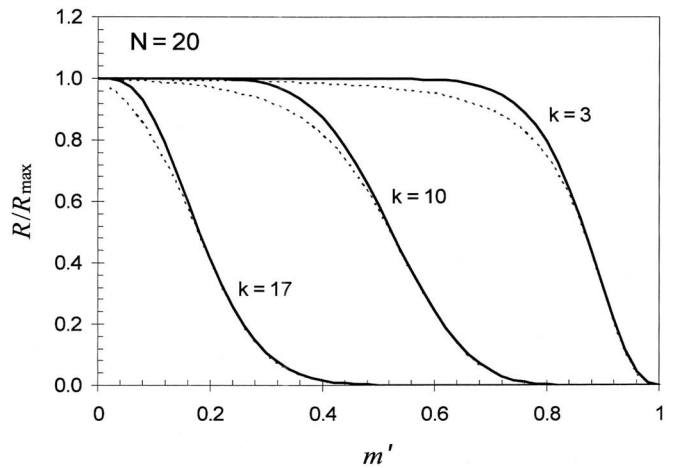
$$n = k[1 + 0.08385(1 - km_{\text{th}})]. \quad (9)$$

These empirical relations are shown as the dotted lines in Fig. 3. To first order,  $n \approx k$ , which matches with the kinetic derivation of the Mack model.<sup>2</sup>

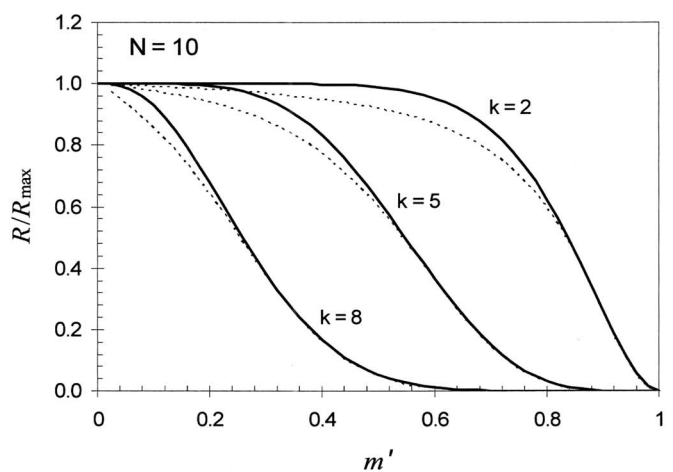
The good match of the Mack model to the CI model (and by extension, the CACI model) in the lithographically significant region of the dissolution-rate curve can be thought of in two ways. Since the Mack model has found wide empirical acceptance with respect to both experimental development rates and the predictive capabilities of simulators using this model, the above comparison serves as empirical justification of the CI model by proxy. Alternately, the theoretical foundation of the CI model and the first-principles meaning of its parameters gives a firmer theoretical footing to the Mack model and, along with Eq. (9), enables a more first-principles interpretation of the parameters  $n$  and  $m_{\text{th}}$ .

#### IV. UNCERTAINTY IN DISSOLUTION RATES

One important advantage of stochastic approaches to modeling is the ability to predict the variance of physical



(a)



(b)

FIG. 2. Comparison of the critical ionization model of Eq. (4) (solid lines) with the original Mack model of Eq. (8) (dotted lines) for different values of  $k$ : (a)  $N=20$  and (b)  $N=10$ . The parameters for the Mack model were found using a best fit to the CI model for  $R < R_{\max}/2$ .

quantities in addition to the mean, something that continuum models cannot do. The stochastic nature of the critical ionization model allows a prediction of the mean development rate, as described in Sec. III, and also the variance of that development rate. Equation (2) gives the probability that a given polymer molecule will be soluble. Recalling the definition of the random binary variable  $y_r$ , the mean value of  $y_r$  and its variance are given by

$$\langle y_r \rangle = P(y_r = 1), \quad \sigma_{y_r}^2 = \langle y_r \rangle (1 - \langle y_r \rangle). \quad (10)$$

The goal now is to relate these properties of  $y_r$  to the development rate. It is tempting to think of dissolution as like any other bulk chemical reaction, where the probability that the polymer is soluble is proportional to the mean-field rate of dissolution. In this approach,

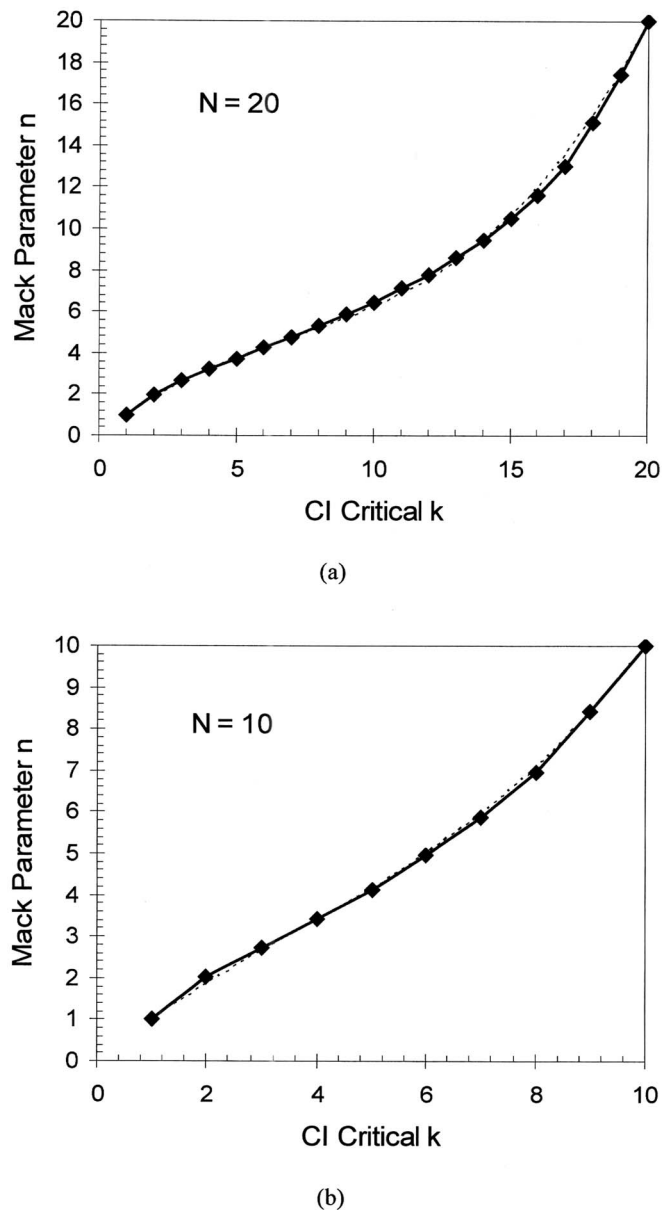


Fig. 3. Best fit Mack dissolution selectivity parameter  $n$  for different values of  $k$  (symbols plus solid line): (a)  $N=20$ , and (b)  $N=10$ . The parameters for the Mack model were found using a best fit to the CI model for  $R < R_{\max}/2$ . Also shown is an empirical fit (dotted line) given by Eq. (9).

$$\langle R \rangle = R_{\max} \langle y_r \rangle, \quad \sigma_R^2 = \langle R \rangle (R_{\max} - \langle R \rangle). \quad (11)$$

Unfortunately, this simple approach leads to a result that does not correspond to experience with line-edge roughness. For example, if  $R_{\max} = 500$  nm/s and the mean  $R$  near the resist line edge is 5 nm/s, Eq. (11) predicts that the standard deviation of the development rate will be about 50 nm/s. The maximum standard deviation of development rate occurs when  $\langle R \rangle = R_{\max}/2$ , giving a standard deviation that is also  $R_{\max}/2$ . These uncertainties would imply a resulting line-edge roughness far in excess of what is observed.

This difficulty is resolved by more carefully defining the meaning of development rate. Rather than development rate as a bulk property of the resist, development rate is best

defined as the velocity of the moving boundary between the resist and developer. Consider the very simple case of a large, open-field exposure so that the mean dissolution front moves vertically through the resist. Letting  $z(t)$  be the depth into the resist of the moving front, then

$$\langle R \rangle = \frac{d\langle z \rangle}{dt}. \quad (12)$$

Nominally, this path of development is perfectly vertical. However, when stochastic fluctuations are included these paths have a random component and are only vertical in the mean. To determine the uncertainty in development rate, the impact of polymer solubility uncertainty on the path of development must be determined. One valuable approach toward investigating the uncertainty in development paths is percolation theory.

## V. DEVELOPMENT AS PERCOLATION

As an illustrative example, percolation describes the flow of fluid through a porous material by means of an interconnected clusters of holes in the material through which the fluid flows. Let  $p$  define the relative density of holes in the material (and thus the probability that any given point in the material will be within a hole). If  $p=1$ , fluid flows unimpeded since the entire material is one big hole. If  $p=0$ , no fluid can flow since there are no pathways in the solid material. While these two extreme cases are obvious, what is less obvious is the existence of a critical pore density,  $p_c$ , below which the distance that a fluid can travel becomes finite. In other words, given an infinitely large block of porous material, for any  $p$  greater than or equal to  $p_c$ , there will always be at least one completely interconnected set of pours that allows fluid to travel an infinite distance through the material. In three dimensions, the value of  $p_c$  depends on the packing structure (lattice) of the material, but is typically in the range 0.15–0.25. A value of 0.2 is often used for a three-dimensional random (disordered) cubic lattice.

As one might expect, the rate at which the fluid flows through the material depends on  $p$ . For  $p \gg p_c$ , the rate is proportional to  $p$ . But as  $p$  approaches  $p_c$ , the rate generally follows a power law:

$$\langle R \rangle \propto (p - p_c)^\beta, \quad (13)$$

where  $\beta$  is related to the fractal dimension of the material and is often estimated to be around 2. For  $p < p_c$ , fluid may penetrate into the material, but eventually its flow comes to a halt.

Many people have applied percolation theory to resist development over the years,<sup>3–9</sup> with mixed results. Given the application of this theory that produced its name, most researchers in this field have thought of development percolation as the penetration of developer through openings in the resist caused by the ionization of the deprotected phenol group,<sup>3–8</sup> though an average deprotection probability over the diffusion length of the acid has also been used.<sup>9</sup> Setting up a percolation grid corresponding to phenol groups, the percolation probability is thus equal to (or at least linearly

related to)  $p_{\text{ion}}$  as defined above for the critical ionization model. In the region as  $p$  approaches  $p_c$ , this leads to<sup>3</sup>

$$R \propto (p_{\text{ion}} - p_{\text{ion-c}})^2 = (p_m - p_{m-c})^2 \propto (\langle m \rangle - m_c)^2. \quad (14)$$

The problem with this percolation approach to dissolution is now clear: dissolution rate is proportional to the relative blocked site concentration to the second power, with no opportunity to explain high-contrast dissolution behavior, nor its dependence on  $N$  or  $l$ . Thus, many previous efforts at using percolation theory to explain dissolution behavior have proven less than fruitful.

A different choice for a percolation description is to consider dissolved polymer molecules as sites within the resist for developer to penetrate. In this view, percolation becomes a stochastic approach in determining the path of dissolution. The probability  $p$  then becomes the probability of polymer dissolution,  $P(y_r=1)$ . As a result, in the high-dissolution-rate region, development rate will be proportional to the probability that a random polymer molecule is soluble. But in the low-dissolution-rate region, development rate (the rate of motion of the boundary between resist and developer) is reduced by the limited pathways available to developer to go around insoluble polymers to keep the front moving.

Mathematically, the percolation behavior as described above could be modeled as

$$\frac{\langle R \rangle}{R_{\text{max}}} = \left( \frac{\langle y_r \rangle - p_c}{1 - p_c} \right)^2, \quad (15)$$

where  $\langle y_r \rangle = P(y_r=1)$  is the probability that a polymer is soluble as given, for example, by Eq. (4) or (7). While this expression is only strictly accurate in the low-dissolution-rate region ( $\langle y_r \rangle$  near  $p_c$ ), since this is the lithographically significant region it will cause little harm to use this expression over the full range of development rates.

Figure 4 shows two plots of the resulting development rate assuming  $\langle y_r \rangle$  can be predicted using the CACI model, using  $p_c=0.2$ . For Fig. 4(a),  $N=10$ ,  $l=8$ , and  $k=4$  in the CACI+percolation model. Also shown in Fig. 4(a) is the CACI model without percolation, but with  $N=13$ ,  $l=13$ , and  $k=6.9$ . Note that the two resulting development curves are virtually indistinguishable, except a small difference near the knee of the curve. For Fig. 4(b),  $N=20$ ,  $l=16$ , and  $k=8$  in the CACI+percolation model. Also shown in Fig. 4(b) is the CACI model without percolation, but with  $N=26$ ,  $l=26$ , and  $k=12.9$ . Again, the two resulting development curves are very close, though the percolation model does drop to lower development rates more quickly at the knee. Thus, the impact of percolation can be seen as an effective increase in the contrast of the development (giving the same performance as a resist with a 30% higher value of  $N$ ).

While adoption of a percolation approach will have an impact on the predicted development performance of a resist with known polymer configuration (that is, known  $N$ ,  $l$ , and  $k$  parameters), the above results show that an empirical development model that ignores percolation should do a good job of describing the dissolution properties of a resist model that includes percolation. The benefit of a percolation view, then,

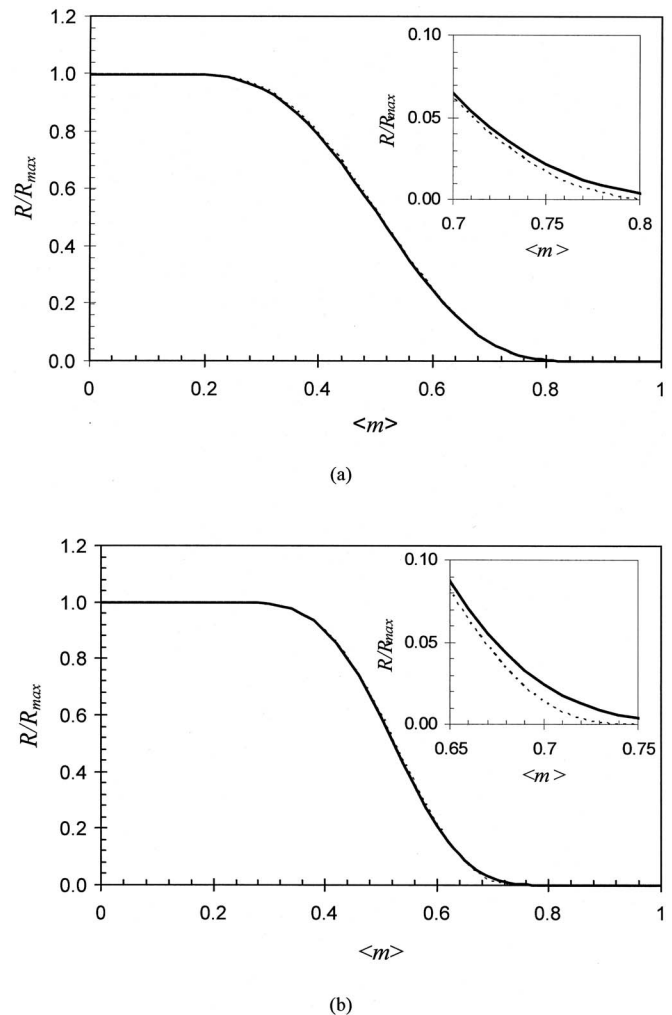


FIG. 4. Comparison of the CACI model with percolation (solid lines) and without (dotted lines), with parameters adjusted to get the best match between the two: (a)  $N=10$ ,  $l=8$ , and  $k=4$  in the CACI+percolation, and  $N=13$ ,  $l=13$ , and  $k=6.9$  in the CACI without percolation; (b)  $N=20$ ,  $l=16$ , and  $k=8$  in the CACI+percolation, and  $N=26$ ,  $l=26$ , and  $k=12.9$  in the CACI without percolation.

should come from its ability to predict development path uncertainty. Note, however, that percolation effects could be an explanation for the “notch” effect—a lower than expected development rate near the knee of the dissolution-rate curve—that has been previously observed.<sup>10</sup>

Consider, as a first case, development in the high-dissolution-rate regime (chosen for the simplicity of the analytic approach that will be taken). Consider the resist as made up of a three-dimensional cubic lattice, each lattice cell consisting of one polymer molecule. In the high-dissolution-rate regime, most polymer molecules are soluble. Figure 5 depicts this case (in two dimensions) where an open cell represents a soluble polymer and an “X” in a cell represents an insoluble polymer.

Our simple case will assume uniform deprotection through the volume, so that development will nominally proceed purely in the  $z$  (downward) direction. For a volume of

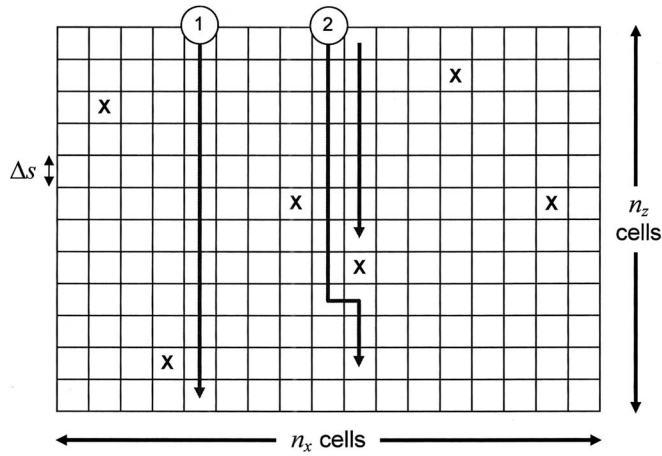


FIG. 5. Schematic representation of a cubic grid of resist polymers (the open grid represents a soluble polymer, and a grid filled with an “X” signifies an insoluble polymer) for the case of a high-dissolution rate. The arrows indicate paths of dissolution.

$n_x \times n_y \times n_z$  cells (letting  $n_x = n_y$ ), where  $a$  of the cells contain insoluble polymers, we have (by the law of large numbers)

$$P(y_r = 1) = 1 - \frac{a}{n_x^2 n_z}. \quad (16)$$

Letting  $\Delta s^3$  be the volume of one cell ( $\Delta s$  will typically be one to a few nanometers), we shall pick a development time  $t_{\text{dev}}$  so that fully deprotected resist will just be removed to a depth  $n_z \Delta s$ :

$$t_{\text{dev}} = \frac{z_{\text{max}}}{R_{\text{max}}} = \frac{n_z \Delta s}{R_{\text{max}}}. \quad (17)$$

Figure 5 also depicts possible development paths through this lattice. If a vertical column of the lattice cells contains no insoluble polymers, then the path of development through those cells will be vertical, reaching the bottom in the allotted development time (labeled as path 1 in Fig. 5). If, however, a path encounters an insoluble cell, it must go around that cell to continue. The principle of least action dictates that the path of least time will be chosen. The path labeled 2 in Fig. 5 will dissolve the cells below the insoluble polymer in the least time, and in the allotted development time will reach a depth of  $z_{\text{max}} - \Delta s$ . If a development path encounters  $i$  insoluble polymers, the depth reached will become approximately  $z_{\text{max}} - i \Delta s$ .

Let us define  $P_i$  as the probability that  $i$  insoluble polymers are encountered over the course of one development path. The resulting mean depth developed will then be

$$\langle z \rangle = \sum_{i=0}^{\infty} (z_{\text{max}} - i \Delta s) P_i = z_{\text{max}} - \Delta s \langle i \rangle. \quad (18)$$

If the mean number of insoluble polymers encountered over one development path is reasonably small (so that they do not interact with each other or “clump” together), its value can be approximated as

$$\langle i \rangle = n_z P(y_r = 0) = \frac{z_{\text{max}}}{\Delta s} (1 - P(y_r = 1)). \quad (19)$$

Defining  $\langle h \rangle = z_{\text{max}} - \langle z \rangle$  as the mean height of the surface above  $z_{\text{max}}$ , we see that

$$\langle z \rangle = z_{\text{max}} P(y_r = 1) \quad \text{and} \quad \langle h \rangle = z_{\text{max}} P(y_r = 0). \quad (20)$$

The mean of the development rate can now be expressed using the definition of development rate as the rate at which the resist/developer interface travels (that is, the speed of the development path). Applying Eq. (12) for this case of “uniform” random deprotection, and using Eq. (20),

$$\langle R \rangle = \frac{\langle z \rangle}{t_{\text{dev}}} = \frac{z_{\text{max}}}{t_{\text{dev}}} \langle y_r \rangle = R_{\text{max}} \langle y_r \rangle. \quad (21)$$

This result shows that the assumptions made (insoluble polymers do not “clump” together) is equivalent to saying that  $\langle y_r \rangle \gg p_c$  and the development has not entered the percolation regime defined by Eq. (13).

Calculating the variance of  $z$  or  $h$  requires some knowledge of the probabilities  $P_i$ . A very common result in percolation problems (as well as in the kinetics of gases and other well-known problems) is that the probability density of path length traveled before encountering an insoluble polymer ( $x$ ) follows an exponential distribution.

$$P(x) = \frac{1}{\xi} e^{-x/\xi}, \quad (22)$$

where  $\xi$  is the mean free path, given by

$$\xi = \frac{z_{\text{max}}}{\langle i \rangle} = \frac{\Delta s}{P(y_r = 0)}. \quad (23)$$

The standard deviation of the exponential distribution is equal to its mean, so that the standard deviation of the development rate is then

$$\sigma_R = \frac{\sigma_z}{t_{\text{dev}}} = (R_{\text{max}} - \langle R \rangle). \quad (24)$$

For the case of dissolution rates near the maximum, this standard deviation is significantly smaller than that given by Eq. (11), which looked at a bulk dissolution independent of path.

The stochastic analysis of the dissolution path described in the above example is extremely limited, examining only the regime of high development rates rather than the more interesting low development rates. However, even in this limited regime we have been able to point out that stochastic variations in development rates must be used to find stochastic variations in the development paths if we wish to use this information to predict surface or line-edge roughness. Further efforts into the more difficult but more interesting regimes of low development rates should lead to a prediction of the influence of development properties on the resulting surface and line-edge roughness of the final resist features. Combining this stochastic description of development rates

and paths with the statistical uncertainty in the amount of deprotection after PEB (Ref. 11) would then lead to a comprehensive LER model.

## VI. CONCLUSIONS

The critical ionization model is valuable for understanding photoresist dissolution because of its ability to predict mean dissolution-rate behavior as a function of photoresist structural properties. Unfortunately, the mathematical form of this model is cumbersome and computationally expensive. In this paper a continuous approximation to the critical ionization model has been derived and shown to match the CI model extremely closely. Further, both of these models were shown to match the widely used Mack model of dissolution over the lithographically significant ranges of development rates. These efforts so far have assumed an idealized photoresist formulation with monodisperse, identical polymers ( $N$  and  $l$  completely fixed). Further work will include distributions of these parameters to determine the effects of such distributions on the mean dissolution rates.

Percolation theory is often invoked to show that stochastic dissolution path effects impact the mean dissolution rate. However, many past efforts have treated polymer ionization sites as percolation sites, leading to predictions of dissolution behavior far different from that observed experimentally. In this paper, it has been shown that choosing the polymer molecule itself as the percolation site leads to development rates consistent with experimental dissolution-rate behavior, and is thus a better candidate for the proper application of percolation theory to resist dissolution. However, the use of percolation theory to predict mean dissolution rates does not lead to a prediction that is easily discernable from bulk dissolution-rate predictions with moderately changed parameters. Thus, the value of percolation theory will undoubtedly come from its use in predicting the variance of dissolution rate.

In order to model line-edge roughness, the variance of dissolution rate must be known in addition to its mean value. However, the variance of the “bulk” dissolution rate is not the critical variance here, but rather that variance in the dissolution front moving through the resist. In other words, variation in dissolution arises from the variation in the development path required to bypass randomly distributed insoluble polymer molecules rather than just the variance in the polymer solubility itself. An analytical treatment of the variance of the dissolution front in the high-dissolution-rate regime has been provided here. This treatment, while insightful, is only a first step toward a fuller understanding of development path variance. In particular, the more interesting regime of low-dissolution rates (such as the dissolution rate at the nominal resist edge) has yet to be addressed and will be the subject of future work. Percolation theory, where the percolation probability is equal to the probability that a polymer molecule will become soluble, has the potential for providing the theoretical framework required to solve this problem, leading to more comprehensive model of LER than is currently available.

<sup>1</sup>P. Tsiartas, L. Flanagan, C. Henderson, W. Hinsberg, I. Sanchez, R. Bonnacaze, and C. G. Willson, *Macromolecules* **30**, 4656 (1997).

<sup>2</sup>C. A. Mack, *J. Electrochem. Soc.* **134**, 148 (1987).

<sup>3</sup>T. F. Yeh, H. Y. Shih, and A. Reiser, *Macromolecules* **25**, 5345 (1992).

<sup>4</sup>T. F. Yeh, A. Reiser, R. R. Dammel, G. Pawlowski, and H. Roeschert, *Macromolecules* **26**, 3862 (1993).

<sup>5</sup>H. Y. Shih, T. F. Yeh, and A. Reiser, *Macromolecules* **27**, 3330 (1994).

<sup>6</sup>H. Y. Shih and A. Reiser, *Macromolecules* **28**, 5595 (1995).

<sup>7</sup>H. Y. Shih, T. F. Yeh, and A. Reiser, *Macromolecules* **29**, 2082 (1996).

<sup>8</sup>A. Yamaguchi, M. Takahashi, S. Kishimura, N. Matsuzawa, T. Ohfujii, T. Tanaka, S. Tagawa, and M. Sasago, *Jpn. J. Appl. Phys., Part 1* **38**, 4033 (1999).

<sup>9</sup>Y. Ma, J. Shin, and F. Cerrina, *J. Vac. Sci. Technol. B* **21**, 112 (2003).

<sup>10</sup>C. A. Mack and G. Arthur, *Electrochem. Solid-State Lett.* **1**, 86 (1998).

<sup>11</sup>C. A. Mack, *Fundamental Principles of Optical Lithography: The Science of Microfabrication* (Wiley, London, 2007), Chap. 6.